Mine Water and the Environment (2022) 41:210–224
https://doi.org/10.1007/s10230-021-00804-z

TECHNICAL ARTICLE

# Environmental Aspects of a Major ARD Source at El Indio Au-Cu-As District, North-Central Chile

**Jorge Oyarzún[1] · Hugo Maturana[2] · Andrzej Paulo[3] · Javier Lillo[4,5] · Pablo Pastén[6,7] · Jorge Núñez[1,8] · Denisse Duhalde[1] · Cinthya González[9] · Adriana Portilla[9] · Ricardo Oyarzún[1,10,11]**

Received: 21 January 2021 / Accepted: 28 July 2021 / Published online: 5 August 2021

**Abstract**

El Indio, an Au-Cu-As deposit with outstanding gold grades, was mined in the Andes of the Coquimbo region, Chile, between 1975 and 2002. Sediment and water sampling of the rivers in the 2000 s found exceptional As and metal levels in modern and old sediments. The studies also revealed that acid rock drainage (ARD) has been present in the district for nearly 10,000 years and the effect that the mining of the district had in terms of geochemical anomalies. The convergence of mineralogical, structural, and hydrologic conditions has generated a metal-rich ARD, a process followed by transference of metals to the fine sediments. In this context, the study also deals with the risk of metal and metalloid transfers from the sediments to the river waters as a consequence of eventual physical-chemical changes, due for example, to climatic-driven conditions. Water and sediment samplings were carried out to provide materials for selective extraction tests under acidic, acid-reducing, and acid-oxidizing conditions. The different behavior of metals and metalloids was revealed and highlighted the refractory character of As. Additionally, the study included the characterization of the sediment's mineralogy, and allowed the detection of new geochemical anomalies of Cu, Zn, Co, and Y in the Incaguaz River, along with high dissolved Li concentrations in the Toro and Turbio rivers.

**Keywords** Coquimbo region · Elqui valley · Hydrothermal Li · Cu-Zn-Co-Y-Anomalies · ARD · Sequential extractions

## Introduction

The El Indio (Au-Cu-As) deposit was well known for its exceptional gold grades (over 200 g $t^{-1}$ in the direct export ore). The El Indio Mining District (EIMD), which included other minor deposits (Jannas et al. 1990, 1999) was exploited between 1975 and 2002. The district is located in the high Andes of Chile's Coquimbo Region, at some 4,000 m above sea level (masl), at latitude 30ºS, in the headwaters of the Elqui river basin; in turn, the watershed is hydrologically connected to the Pacific Ocean via the Elqui River (Fig. 1). Given the existence of the EIMD, the Elqui river basin has become a valuable natural laboratory for the study of the dynamics of metals and metalloids in mountain rivers. This

---

✉ Ricardo Oyarzún
royarzun@userena.cl

[1] Departamento Ingeniería de Minas, Universidad de La Serena, La Serena, Chile

[2] Escuela de Ingeniería en Prevención de Riesgos y Medio Ambiente, Universidad Católica del Norte, Coquimbo, Chile

[3] AGH University of Science and Technology, Krakow, Poland

[4] Departamento de Biología, Física y Química Inorgánica, Escuela Superior de Ciencias Experimentales y Tecnología, Universidad Rey Juan Carlos, Tulipán s/n, 28933 Móstoles, Madrid, España

[5] IMDEA Agua, Avda. Punto Com, N°2, 28805 Alcalá de Henares Madrid, España

[6] Departamento de Ingeniería Hidráulica y Ambiental, Pontificia Universidad Católica de Chile, Santiago, Chile

[7] Centro de Desarrollo Urbano Sustentable, Santiago, Chile

[8] Centro del Agua para Zonas Áridas y Semiáridas de América Latina y el Caribe, La Serena, Chile

[9] Licenciatura en Química, Universidad de La Serena, La Serena, Chile

[10] Centro de Recursos Hídricos para la Agricultura y la Minería, Concepción, Chile

[11] Centro de Estudios Avanzados en Zonas Áridas, La Serena, Chile

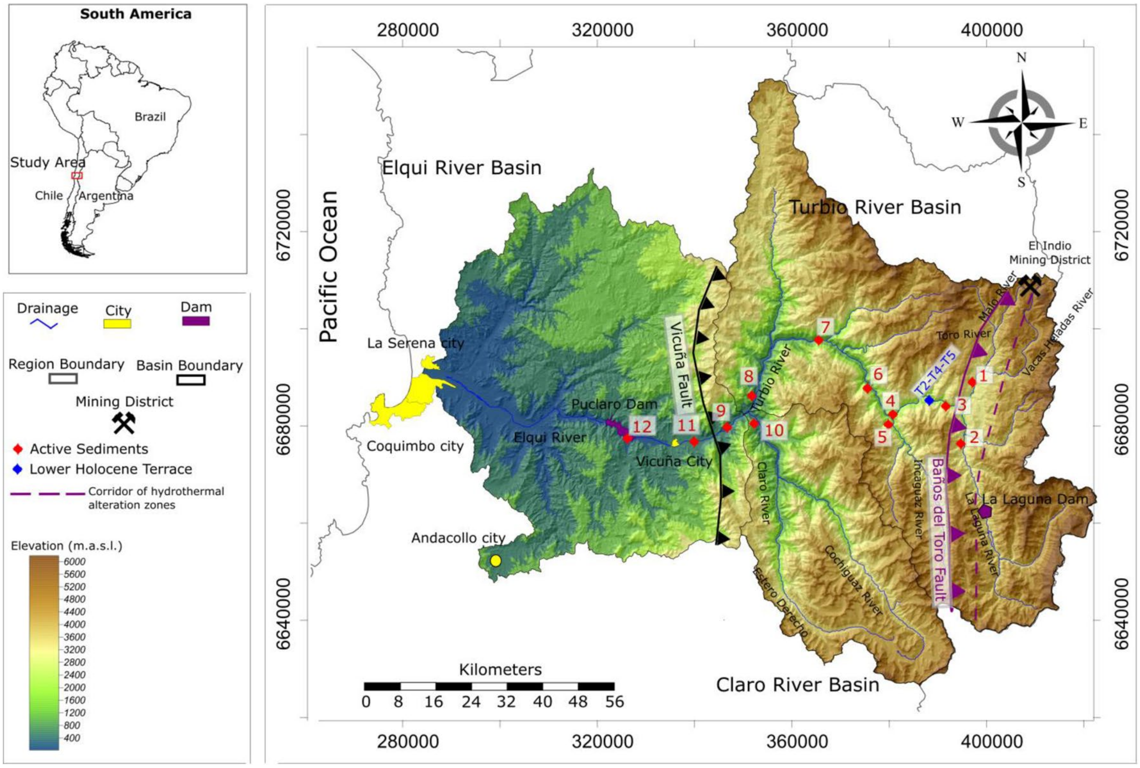

**Fig. 1** The Elqui river basin, main structural traits, and sampling locations (1: Toro River; 2: La Laguna River; 3, 4, 6, 7, 8, 9: Turbio River; 5: Incaguaz River; 10: Claro River; 11, 12: Elqui River; T2, T4, T5: Lower Holocene Layer samples)

issue is receiving increasing attention as toxic elements are mobilized from natural and mining sources in the basin's headwaters to downstream valleys with agriculture and/or urban water requirements (e.g. Bugueño et al. 2014; Guerra et al. 2016; Montecinos et al. 2020).

Fine-sediment sampling carried out in 2000 throughout the Elqui basin revealed high levels of Cu, Zn, and As in the Toro, Turbio, and Elqui rivers, with Cu concentrations (1000 ppm average) being of higher magnitude than those of Chile's other rivers with copper deposits (Oyarzún et al. 2003). Later, a geochemical study allowed us to discriminate the contribution of mining and metallurgical operations to metals and metalloids concentrations in river waters (Oyarzun et al. 2006). More recently, both surface waters and groundwaters were studied to obtain a general understanding of the factors and mechanisms determining their chemistry and isotopic compositions (Oyarzún et al. 2013).

The Elqui river is very important in the region because: (1) of the agricultural activity, with fruits such as table grapes destined to foreign markets; and (2) the cities of Vicuña and La Serena-Coquimbo conurbation (ca. 430,000 inhabitants) depend on the Elqui River for most of their water needs. New water and sediment mineralogical and chemical data were collected, and sequential extractions were performed to assess the environmental implications of ARD generation in the EIMD area.

## Characteristics and History of the El Indio Mining District (EIMD)

### General Geographic and Geological Context

The EIMD is located between 4000 and 4150 masl in the Andes mountains, in the NE headwaters of the Elqui River basin (9645 km$^2$), at latitude 30 °S, where Chile is just 137 km wide (Fig. 1). Precipitation in the basin presents strong altitudinal dependence, with an orographic gradient in the basin of ca. 22 mm/km (Scaff et al. 2017). Therefore, average annual precipitation ranges from ≈ 80 mm on the coastline to 140 mm inland at 1000 masl, and attains 200–300 mm at the higher realm in the Andes Cordillera (Favier et al. 2009). There is also important inter-annual precipitation variability (Núñez et al. 2013). In consequence, streamflows are rather low, and highly variable. They increase in winter (June–August) when it rains in the middle and lower parts of the basin, but peak discharges occur in late spring-early summer, when the snowpack melts.

The main rivers are the Toro and La Laguna rivers, which converge into the Turbio River; downstream, the latter receives waters from the Incaguaz and Claro rivers, eventually becoming the main Elqui River. These rivers are perennial, although their long-term flow show important variations during the year; Toro River: 0.5–1.5 $m^3s^{-1}$; La Laguna River: 1–5 $m^3s^{-1}$; Turbio River, 4–13 $m^3s^{-1}$; Incaguaz River, 1–2 $m^3s^{-1}$; Claro River, 3–11 $m^3s^{-1}$; and Elqui River, 6–24 $m^3s^{-1}$. The basin has two dams: the 40 $Mm^3$ capacity Laguna dam built in 1937 and the 200 $Mm^3$ capacity Puclaro dam, built in 2000, in the Elqui River (Fig. 1) (Galleguillos et al. 2008).

The structural control of the topography exerted by a major N-S trending reverse fault results in river gradients (slopes) of up to 7% in some sections (Zavala 2006). Thus, river streamflows are rather torrential, with a capacity to move and transport different sediment fractions, even up to the size of cobbles.

The general geology of the Elqui River basin is dominated by calc-alkaline plutonic, volcanic, and volcano-sedimentary rocks of Paleozoic to Cenozoic age. The current tectonic regime is compressive and no Quaternary volcanic rocks are present. The stratified rock formations and structural alignments are parallel or sub-parallel to the N-S subduction zone that has controlled the post-Paleozoic magmatism of the western edge of Chile (Maksaev et al. 2007). Manto-type and vein Cu and Ag deposits are scattered throughout the basin. They have low sulfur/metal ratios and are associated with propylitic alteration (Oyarzun et al. 1998), and are not sources of acid drainage. The eastern realm (hosting the El Indio gold deposits) is characterized by the presence of Cenozoic volcanic and subvolcanic rocks and Permian granitic plutonic bodies.

The El Indio deposit is located at the onset of the Toro River at latitude 30 °S, near the boundary with Argentina. The ore deposit is associated with Miocene dacitic intrusives and is about 10 Ma old. The district includes two other smaller, nearby deposits: Tambo and Río del Medio (Jannas et al. 1999). The structural setting of this eastern realm is characterized by the existence of major NNW oriented swarms of large-scale faults of Oligocene age. During the Miocene, these acted as structural channels for the results of the volcanic and subvolcanic magmatic activity (and related hydrothermal phenomena) at the highest levels (Oyarzun et al. 2007a).

## ARD Generation and Geochemical Anomalies in the El Indio Mining District

The district is located along a N-S (150 × 10 km) belt characterized by varied and intense colors (red, yellow, green, etc.) resulting from the hydrothermal and supergene (ARD) alteration of rocks (Fig. 1). This highly altered surface (a large part being a regolith flanking the hills) and its metal- and As-rich ARD is explained by the confluence of several conditions. First, most of the mineralization of the El Indio deposit was concentrated within a 300 m deep, 500 × 150 m block, which is thought to have undergone only moderate (≈ 200 m) unroofing (Bissig et al. 2003). This extraordinary spatial concentration of mineralizing processes also explains the remarkable gold grades. Maksaev et al. (2007) estimated that a third of the extracted ore had a grade of 209 g $t^{-1}$ Au and one vein reached 3500 g $t^{-1}$ Au.

El Indio is a high-sulfidation deposit characterized by widespread presence and overprinting of: (1) massive veins of enargite-pyrite-alunite and alunite-quartz with native sulfur in the upper levels of the body (copper stage) and (2) Au-quartz ore (gold stage). The hydrothermal alteration and related geochemical anomalies help explain the variable potential of the sulfide deposits to generate ARD. For instance, the large porphyry copper deposit of Los Pelambres (Reich et al. 2013), ca. 200 km south of the EIMD and associated with moderate hydrothermal alterations (i.e. propylitic, silicic, and potassic), has produced only weak geochemical anomalies in the Choapa River basin (Oyarzun et al. 2007b; Parra et al. 2011). Likewise, the Río del Medio deposit (EIMD), linked to propylitic alteration in andesitic rocks, did not generate ARD, despite being surrounded by zones of advanced alteration (Maturana et al. 1995).

A second important factor is the complex structural fracture network that hosts the multiple vein clusters associated with a regional flexure of the N–S magmatic arc, intersected by an ESE structural corridor (Heather et al. 2003). This resulted in the presence of structural blocks separated by multidirectional faults (NE, N, NW, and ESE), facilitating the generation and transport of ARD. The hydraulic gradient caused by the block tectonic and the post-glacial topography has also provided a continuous groundwater flow, controlled by the annual snow precipitation followed by thawing during the spring-summer period. In this regard, ARD generation has been enhanced by the underground openings remaining after closure of the mine.

Except for the strip of hydrothermal alterations and pyrite oxidation in the EIMD, there are no other ARD sources in the Elqui river basin, nor are other known sources of Cu, As, and Zn that can explain the described anomalies (Oyarzun et al. 2007a). On the other hand, the mixing of the acidic water of the Toro River (pH 4–5) with the alkaline water of the La Laguna River (pH 7.5–8) neutralizes the ARD, and causes the dissolved metals (Cu, Fe, Zn, etc.) to precipitate as fine sediments. This also explains why the Toro River is the only one whose waters reach Cu concentrations on the order of 10 ppm. The As co-precipitates/adsorbs to the $Fe(OH)_3$ phase. The alkalinity of the Turbio and Elqui river water is subsequently enhanced by the inputs of the Incaguaz and Claro rivers.

Regarding the onset of metal and metalloid input, Narváez (1970) indicated anomalous contents of Cu, Fe, As, and Mo near the El Indio deposit and in the Turbio River headwaters. However, the confirmation of significant geochemical anomalies long before mining arose from the discovery of a metalliferous gypsum and carbonaceous layer in a terrace of the Turbio River, 5 km downstream of the confluence of the Toro and Laguna rivers (Oyarzun et al. 2004). The sampling of this layer, about 3 m thick, indicated average contents of 3593 ppm Zn, 697 ppm Cu, and 749 ppm As, and a $^{14}$C age of 9640 ± 40 years. This Lower Holocene layer (LHL) was likely deposited at the bottom of a temporary water reservoir such as a small lake, formed during the initial meltdown of glaciers. Thus, the presence of these As-metal rich sedimentary beds indicates that ARD generation was taking place at least ca. 10,000 years ago.

## Mining of the District, Post-closure Measures, and Geochemical Implications

The mining of El Indio started in 1975, when most of the property was acquired by St. Joe Minerals. The presence of high-grade gold ores (over 200 $gt^{-1}$) allowed the direct shipping of run-of-mine ore minerals (DSO: "direct shipping ore"), with a profitable return. During this period, detailed geochemical studies of the site were carried out, revealing an elevated As concentration in thealtered rocks and soils (regolith), which included large areas with over 3500 ppm As. Since 50% of the gold mineralization was associated with enargite, a prior ore roasting process was required for ores under the DSO grade, which generated fine-particulate $As_2O_3$ pollution (Maturana et al. 1996).

Subsequently, the district underwent various ownership changes. Barrick, the last owner, ceased mining there in 2002. Maksaev et al. (2007) estimated that the total production in those ca. 20 years reached 126 t of Au, 630 t of Ag, and 0.32 Mt of Cu, rather moderate figures considering the high ore grades.

An important issue complementing the origin and age of the anomalies is the extent to which mining operations in the EIMD contributed to their intensification and to ARD-related metal dispersion. This was addressed by Oyarzun et al. (2006) using information provided by the DGA (Chilean Water Authority) for the 1975–1995 timeframe. They described a sustained increase of total As, Cu, and Fe concentrations in the Turbio River waters. Arsenic increased from 0.05 to 0.33 $mgL^{-1}$ (66 times), Cu from 0.02 to 2.0 (100 times), and Fe from 2.62 to 7.10 $mgL^{-1}$ (2.7 times). Thus, it is clear that mining operations at the EIMD increased the metal contents of the water and fine sediments of the Toro, Turbio, and Elqui rivers.

The closure operations were important for several reasons. First is the location of agricultural lands and a town (Vicuña, 13,000 inhabitants) along the Elqui River course, and an important conurbation at its mouth (Coquimbo-La Serena, 415,000 inhabitants), which depend of the Elqui River water. A second reason is that El Indio was the first planned, voluntary closure of a mine in Chile, implying a significant investment (over U.S. $50 million). A third reason is the geological complexity of the site, given the previously described mineralogical, geochemical, structural, and hydrological characteristics of this realm. Among other actions, portals to the underground mine were closed. Nonetheless, water continued to seep into the partially flooded underground works due to the high degree of rock fracturing and strong hydraulic gradient of the area. Therefore, ARD generation continues. A more recent study (Oyarzún et al. 2018), again based on DGA monitoring data, compared the average Cu, Fe, and $SO_4$ concentrations of the Toro river waters in the 2007–2016 period with that of the 1996–2006 time span. These authors found that Cu had decreased from 17 to 10.5 $mgL^{-1}$ and Fe from 20.4 to18.5 $mgL^{-1}$. However, $SO_4$ increased from 943 to 1102 $mgL^{-1}$, whereas As (0.5 $mgL^{-1}$) did not change, and the pH slightly decreased (4.8 to 4.6).

An unexpected beneficial effect of an activity carried out almost in parallel (but completely independently) to the El Indio closure plan was the construction of the Puclaro Dam, located between Vicuña and La Serena (Fig. 1). The existence of the dam brought a near 50% decrease in As, Cu, and Fe concentrations in the Elqui river waters downstream (Galleguillos et al. 2008). This was attributed to the settling effect associated with the residence time of the water in the dam, most likely facilitated by the sorption of metals in clay or Fe-Mn oxide colloidal particles. This observation highlights the fact that planning of water infrastructures should include geochemical studies and monitoring to assess the potential effects of reservoirs on the transport and fate of metals and metalloids. In fact, the Chironta dam, under construction in the Lluta River, northern Chile, another Andean watershed impacted by ARD, is expected to become a reservoir of fine-grained arsenic sediment (Contreras et al. 2015).

## Elemental Mobility Assessment in Fine Sediments

### Scope of the Study

Elemental mobility of mineral wastes from former mining operations is critical for environmental risk assessments in the post-closure stage (Brown et al. 2017; Caraballo et al. 2018; Nordstrom 2011). In the case of El Indio, this analysis should have also considered the highly anomalous metal contents of the fine sediment fractions of the Turbio and Elqui rivers, as well as those likely to be deposited in the

Puclaro dam. Metals and As may be present in a variety of chemical forms, adsorbed to clay minerals or to Fe- and Mn-oxides and hydroxides, etc. Although it may be difficult to identify the precise chemical species, that determination is very important in evaluating their relative mobility at different environmental conditions, due to local events or regional climatic/hydrological changes. Such assessments can be performed using sequential extraction tests.

To accomplish this, a new sampling of sediments and waters of the rivers of the upper Elqui basin was carried out. The study included XRD mineralogical determinations and ICP-OES spectrographic analysis of fine sediments, and chemical analysis of water. This allowed a more complete mineralogical characterization of the sediments, as well as an increase in the spectrum of elements considered, given the broad analytical range that ICP-OES offers. The sequential chemical extractions from sediment samples (the main driver of the new sampling campaigns) followed a modified BCR (Community Bureau of Reference) procedure (Copaja et al. 2014), simulating the effects of acidic, acid-reducing and -oxidizing conditions on the sediment's metals stability.

## Sampling Campaigns and Sediment Samples Pre-processing

Water and active (i.e. in permanent contact with the river flow) sediment samples were taken in 12 selected locations throughout the drainage network of the upper Elqui River basin (Fig. 1). These sediment samples were obtained from the first 10 cm of the streambed beneath the water column, along a distance of ≈ 20 m, representing an area of ca. 3 $m^2$ (depending on the availability of fine sediments in the transect). Sampling campaigns were held in Sept. 2018 and Jan. 2019 (the latter to verify water and sediment chemical compositions). Field determinations of pH and electrical conductivity of water were conducted at each sampling site. For the Sept. 2018 campaign, three sediment samples were taken from the 9,640-year-old terrace (LHL) identified and studied by Oyarzun et al. (2006). Sediment samples were dried at room temperature in the University of La Serena (ULS) laboratory, after major clastic and organic fragments were discarded by coarse sieving. The fine sediment fraction passing a 63 µm sieve was collected, as it concentrates most of the organic matter and metals (Copaja et al. 2014; Nowrouzi and Pourkhabbaz 2014). Sediments were quartered and stored in clean coded plastic bottles (4 g), each with a counter-sample, for chemical composition analysis. One sample (from site 1) was distributed and stored in 12 differently coded bottles, to have an independent measurement of the laboratory's spectrographic analytical precision (Table 1). It was observed that 18 elements presented coefficients of variation (CVs) of less than 5%; 7 between 5 and 10%, and only 4 above 10% (Ba, Ni, Cu, and Cd). Finally, about 10 g of each sample were saved for x-ray diffraction (XRD) analysis.

## XRD Studies

Powder XRD analyses were carried out using a Bruker D8 Advanced diffractometer for polycrystalline samples, and quantified in accord with the Bruker and COD databases using Topas V5 software at the SAX analytical services laboratory (Santiago, Chile). Samples were powdered at ambient moisture with ethanol to 5–10 µm and compacted on polished glass angular scanning from 3 ° to 80 °, with an analysis time of 35 min. This method identifies crystalline minerals above ≈ 1 % by weight.

## Water and Sediment Chemical Analysis

*Water* As in previous studies (e.g. Oyarzun et al. 2006, 2013), water chemical sampling and analytical procedures were equivalent to those used by the DGA (Chilean Water Authority). The analyses included Li, Na, K, Mg, Ca, Mn, Fe, Cu, Zn, Al, As, $SO_4$, $HCO_3$, $NO_3$, and $PO_4$, and were performed at the Geoquímica analytical services laboratory (Coquimbo, Chile). The laboratory follows "Standard Methods for Examination of Water and Wastewater" (Rice et al. 2017), complemented by Chilean standard NCh 2313-10. The analyses of metals and metalloids were performed using atomic absorption, and ICP scanning for Li. Finally, $PO_4$, $NO_3$, and $SO_4$ were analyzed by colorimetry, uv spectrometry, and gravimetry, respectively.

*Sediments* The ICP-OES analysis of sediment samples were performed by Activation Labs, Coquimbo, Chile, using an Agilent 700 Series radial equipment. The samples

**Table 1** Analytical coefficient of variation (CV = 100*standard deviation/average)

| Element | | | | | | | | | |
|---|---|---|---|---|---|---|---|---|---|
| Na | K | Be | Mg | Ca | Sr | Ba | Se | Sc | Y |
| 2.4 | 3.0 | 5.1 | 1.7 | 2.2 | 2.3 | 20.5 | 0.0 | 0.0 | 7.1 |
| La | Ti | Zr | V | Cr | Mo | Mn | Fe | Co | Ni |
| 2.4 | 4.0 | 5.3 | 2.1 | 3.2 | 7.4 | 4.9 | 2.1 | 8.3 | 11.1 |
| Cu | Zn | Cd | B | Al | Pb | P | As | Sb | S |
| 13.4 | 8.0 | 30.6 | 3.9 | 2.7 | 2.2 | 1.4 | 3.3 | 6.2 | 2.0 |

**Table 2** Mineralogical composition (%) of the sediments

| | Active sediments | | | | | | | | | | | Lower Holocene Layer | | |
|---|---|---|---|---|---|---|---|---|---|---|---|---|---|---|
| | 1 | 2 | 3 | 4 | 6 | 7 | 8 | 9 | 10 | 11 | 12 | T-2 | T-4 | T-5 |
| Feldspar | 50.3 | 42.1 | 35.8 | 36.4 | 38.4 | 38.7 | 42.7 | 45.0 | 54.0 | 63.6 | 49.1 | 32.3 | 30.7 | 26.0 |
| Pyroxene-Amphibole | 3.6 | 0.9 | 1.4 | 1.1 | 1.3 | 0.7 | 0.9 | 3.4 | 4.6 | 1.6 | 3.0 | 0.6 | 0.5 | 0.2 |
| Micas | 2.1 | 10.8 | 13.7 | 12.7 | 13.3 | 12.8 | 11.8 | 10.6 | 3.2 | 6.6 | 8.5 | 9.9 | 6.9 | 13.7 |
| Chlorite | 18.9 | 11.2 | 9.9 | 8.9 | 8.3 | 11.1 | 9.9 | 10.2 | 9.9 | 6.7 | 10.8 | 25.9 | 33.7 | 33.1 |
| Clay minerals | 4.6 | 4.7 | 10.7 | 10.4 | 9.1 | 9.7 | 8.9 | 6.5 | 4.3 | 4.9 | 5.7 | 7.2 | 8.4 | 4.4 |
| Zeolites | 3.8 | | | | | | | | | | | 0.49 | | 4.2 |
| Quartz | 14.1 | 20.5 | 9.6 | 26.2 | 25.7 | 25.1 | 24.4 | 21.9 | 22.1 | 15.8 | 19.0 | 14.8 | 14.1 | 13.0 |
| Hematite | 0.5 | 2.1 | 2.0 | 1.3 | 1.6 | 0.6 | 0.8 | 1.7 | 1.2 | 0.2 | 1.7 | 1.5 | | 0.1 |
| Gypsum-anhydrite | 1.9 | 0.13 | 0.18 | 0.95 | 1.18 | 0.73 | 0.19 | 0.73 | 1.51 | 0.10 | 0.54 | 1.2 | 2.4 | 7.0 |
| Rutile | 0.28 | 0.45 | 0.45 | 1.61 | 0.9 | 0.56 | 0.31 | 0.23 | 0.28 | 0.50 | 0.66 | | 0.31 | 0.2 |
| Calcite | | 7.09 | | | | | | | | | | | | |
| Pyrite | | | 0.37 | 0.37 | 0.25 | 0.07 | 0.20 | | | | | | | |
| Jarosite | | | | | | | | | | | | | | 2.3 |
| Cu sulfate | | | | | | | | | | | | | | 0.61 |

(0.25 g) were digested with aqua regia for 2 h at 120 $^{o}$C in three stages (80$^{o}$, 100$^{o}$, and 120$^{o}$). Then samples were submitted to a second digestion with HCl for 1 h at 80$^{o}$ C. Finally, they were analyzed for 37 elements (Ag, Al, As, B, Ba, Be, Bi, Ca, Cd, Co, Cr, Cu, Fe, Ga, Hg, K, La, Mg, Mn, Mo, Na, Ni, P, Pb, S, Sb, Sc, Sr, Te, Ti, Tl, U, V, W, Y, Zn, and Zr). The QC included duplicate samples, three certified reference materials, and a blank. Given that concentrations of Ag, Bi, Ga, Hg, Te, Tl, and U were below detection limits, they were excluded from subsequent data analyses.

## Sediments Sequential Extraction Analysis

The method simulated the successive effects of different environmental conditions on the metal contents of active sediments in the rivers of the basin and in the LHL, giving an estimate of the potential mobilization resulting from different physicochemical settings. We followed a modified BCR method (Copaja et al. 2014), as our approach involved the analysis of the residual solid fraction from each stage (instead of the leached fraction). This method allowed the use of the same analytical procedure (ICP-OES) to determine the initial concentration in the sediment as well as the resulting concentration from the three successive chemical extractions. The sequential extraction scheme is based on the premise that the exchangeable metal fractions associated with carbonates are extracted by acidic solutions, those bound to Fe and Mn oxyhydroxides by reducing solutions, and those bound to organic matter and sulfides are mobilized at oxidizing conditions.

The following procedure was carried out at the ULS laboratory: Four 2 g aliquots of each sediment sample were subjected to the sequential extraction process; (i) Stage (1) The samples were stirred in 80 mL of 0.11 M acetic acid (pH 2) for 16 h. Then they were centrifuged at 3000 rpm for 40 min and the residue was washed and centrifuged for 20 min. The residue was dried at 40 °C and stored for analysis in polyethylene bottles; (ii) Stage (2) Following the procedure of Stage 1, the solid residues were then treated with 80 mL of 0.1 M hydroxylamine chloride solution (pH 2). They were agitated for 16 h and then centrifuged for 40 min, dried, and stored for analysis; (iii) Stage (3) The solid residues resulting from Stage 2 were treated with 20 mL of hydrogen peroxide (30%) in Erlenmeyer flasks, with intermittent agitation, and then placed in a water bath at 85 °C for 1 h and evaporated to 3 mL. The procedure was repeated with 20 mL of the same reagent at the same temperature and the samples were dried. Ammonium acetate (80 mL) was added and the samples were agitated for 16 h. Finally, the residues were centrifuged, washed with distilled water, centrifuged again for 20 min, dried at 40 °C and stored for analysis. After each stage, two ≈ 4 g composite samples were produced by mixing two subsamples, and were coded and sent as duplicates for chemical analyses; the results of both analyses were averaged. The analysis of results considered 18 elements that allowed determinations with adequate analytical uncertainty as well as sufficient concentration in the sediments.

For a given stage "i", the extraction percentage ($E_i$) was calculated as $E_i = [(C_{i-1} - C_i)/ C_{i-1}]\ 100$, where $C_{i-1}$ is the concentration obtained as a result of the prior stage (or the original content $C_o$ in the case of the first extraction stage) and $C_i$ that of the solid residue resulting from the stage in consideration. Thus, an average $E_i$ for each element was

**Table 3** Average water constituents concentration ($mgL^{-1}$, except Liand As in $mgL^{-1}$) ofthe Elqui basin rivers, and pH and discharge (Q, in $m^3/s$) of theSeptember 2018 sampling campaign (n: number of samples)

| Study | Set | Constituent | | | | | | | | | | | | Parameter | |
|---|---|---|---|---|---|---|---|---|---|---|---|---|---|---|---|
| | | Li | Na | K | Mg | Ca | Mn | Fe | Cu | Zn | Al | As | $SO_4$ | pH | Q |
| Current one | All samples | | | | | | | | | | | | | | |
| | Avg | 254 | 45.5 | 3.75 | 18.8 | 88.7 | 0.91 | 1.74 | 1.87 | 0.40 | 4.86 | 66.1 | 290 | | |
| | StD | 220 | 28 | 2.81 | 11.1 | 52.1 | 1.46 | 2.41 | 3.3 | 0.64 | 7.5 | 83.3 | 275 | | |
| | P50 | 196 | 40 | 3.0 | 16.6 | 83 | 0.48 | 1.14 | 0.83 | 0.21 | 2.64 | 42.6 | 228 | | |
| | IQR | 280 | 25.6 | 1.91 | 8.5 | 32.8 | 0.85 | 1.26 | 1.8 | 0.36 | 4.5 | 70.4 | 137 | | |
| | *Group 1* | | | | | | | | | | | | | | |
| | Toro (n = 1) | 806 | 113 | 11.4 | 49.3 | 236 | 5.33 | 9.0 | 11.9 | 2.33 | 27.5 | 306 | 1099 | 5.0 | 0.4 |
| | Turbio (n = 5) | 336 | 56.5 | 4.3 | 21.1 | 91.4 | 0.91 | 1.8 | 1.8 | 0.40 | 4.9 | 78.5 | 313 | 7.7–8.0 | 4.0 |
| | Elqui (n = 3) | 143 | 34.3 | 2.95 | 14.7 | 81.7 | 0.33 | 0.9 | 0.51 | 0.14 | 1.7 | 25.6 | 197 | 8.1–8.8 | 5.5 |
| | *Group 2* | | | | | | | | | | | | | | |
| | Laguna (n = 1) | 80 | 24.5 | 1.23 | 12 | 55 | 0.031 | 0.16 | 0.013 | 0.016 | 0.1 | 10.6 | 83.1 | 7.6 | 0.9 |
| | Incaguaz (n = 1) | 36 | 12.8 | 1.08 | 8.3 | 39.7 | 0.074 | 0.35 | 0.047 | 0.04 | 0.68 | 3.75 | 78.1 | 8.3 | 0.5 |
| | Claro (n = 1) | 11 | 10.3 | 1.04 | 6.0 | 31.4 | 0.015 | 0.26 | 0.006 | 0.008 | 0.15 | 4.16 | 64 | 8.7 | 2.2 |
| | *Group 1/Group 2* | 10.2 | 4.2 | 5.6 | 3.2 | 3.2 | 55 | 15 | 214 | 46 | 22.4 | 22.4 | 7.1 | | |
| Oyarzún et al. (2013) | Toro (n = 1) | | 82.4 | 10.5 | 40.4 | 196 | 0.8 | 17.6 | 15.8 | 2.58 | 12.5 | 80 | 1045 | | |
| | La Laguna (n = 1) | | 29.6 | 1.5 | 10.5 | 47.2 | 0.04 | 0.21 | na | 0.06 | 0.17 | 20 | 138 | | |
| | Turbio (n = 5) | | 33.0 | 3.1 | 20.0 | 67.6 | 0.76 | 4.1 | 2.2 | 0.40 | 5.6 | 20 | 271 | | |
| | Elqui (n = 8) | | 32.1 | 2.0 | 10.5 | 62.4 | 0.12 | 0.8 | 0.37 | 0.08 | 1.3 | 10 | 169 | | |
| World average (Levinson 1974) | | | 63 | 2.3 | 4.1 | 15 | 0.007 | 0.23 | 0.007 | 0.02 | 0.3 | 2 | 11.2 | | |

Avg: average; Std:standard deviation; P50: median (percentile 50); IQR: Interquartile range (Percentile75-Percentile 25). Reference figures are also included

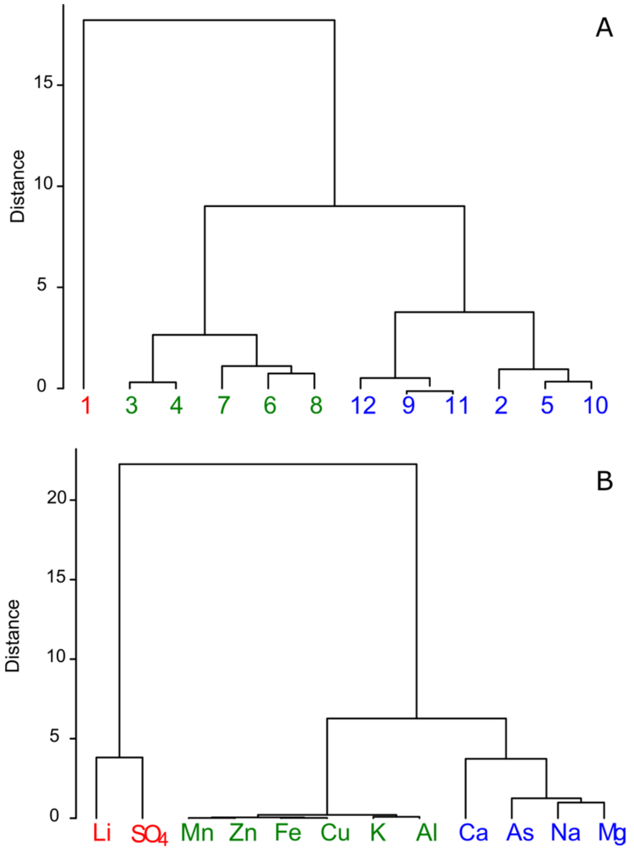

**Fig. 2** Cluster diagrams for water samples composition based on sampling sites (**A**) and elements (**B**)

obtained separately for the active and LHL sediment samples (for calculation purposes, when $E_i$ was 4% or lower, it was computed as 2%).

The total extraction percentage ($E_T$) was the difference between the initial sample concentration ($C_o$) and that measured after the third extraction ($C_3$) (i.e., $E_T = [(C_o - C_3)/C_o] \times 100$). At first, it was assumed that this difference should correspond to the sum of the three extractions ($E_1+E_2+E_3$). However, deviations of up to 10 to 20% were observed in some cases between $E_T$ and $E_1+E_2+E_3$. Therefore, the figures of the three stage extractions were adjusted proportionally. For example, if the total calculated extraction ($E_T$) was 81% and the partial values ($E_1$, $E_2$, $E_3$) were 20, 40, and 30%, the latter were readjusted to 18, 36, and 27%, respectively. This was done to compare the response of the elements to the three types of selective dissolution.

## Results and Discussions

### Water and Sediments Characterization

*XRD study*. The results of the XRD analysis of the active and the Lower Holocene Layer (LHL) sediments are presented in Table 2. The dominant minerals in the active sediments and their average concentration are: feldspars (ca. 45%), quartz (20.4), chlorite (10.5), micas (9.6%), and clays with halloysite dominant (7.2%). Gypsum and anhydrite were found in all the samples, but are more abundant in the LHL (3.5% in average). By contrast, calcite was detected only in the Laguna River sample. The scarcity of calcite was also expressed by a weak or null reaction of the fine sediments to HCl. Meanwhile, zeolites were found only in the Toro River sediment and in two of the three LHL samples. In the latter, copper sulfate and jarosite were also detected. Hematite was present in all the active sediment samples, with an average of 1.2%, but reaches only 0.5% in the LHL, which, in contrast, is rich in chlorite minerals (over 25%).

*Water and sediment chemical data.* The water chemistry data, along with comparative figures, are presented in Table 3. There are striking differences between the high concentrations of the Toro, Turbio, and Elqui rivers and those of the La Laguna, Incaguaz, and Claro rivers. These differences are not related to regional lithological factors, because the original composition of the rocks throughout the basin is rather homogeneous (Oyarzún et al. 2016). Instead, they are due to minor chemical weathering explained by the aridity of this realm and the lack of an ARD imprint on the La Laguna, Incaguaz, and Claro river subbasins. Thus, the average concentrations of the Laguna, Incaguaz and Claro rivers approach the figures proposed by Levinson (1974) for the world`s rivers composition. An interesting finding is that the Li content of the Toro River (800 $\mu gL^{-1}$) is far above the world average (less than 20 $\mu gL^{-1}$) cited by Kavanagh et al. (2017) or the 85 $\mu gL^{-1}$ average determined by Tapia et al. (2018) for Andean rivers of the neighboring Atacama region. Confirming these geochemical relationships, a Q-mode cluster analysis (Fig. 2A) separates the Toro River sample (1) from those of the southern tributaries (La Laguna, Incaguaz, and Claro; 2, 5, and 10, respectively). Two groups are in between, the: a) Turbio (3, 4, 6, 7, 8) and Elqui (11, 12) samples, the latter including the westernmost sample of the Turbio River (9). The elements cluster (R-mode, Fig. 2B) defines one group constituted by $SO_4$ and Li, and a second group for the rest of the elements. Within the latter, two

**Table 4** Chemical compositions of the sediments used in the selective extractiontests (September 2018 sampling campaign, SC-1)

| SC-1 | Na (%) | K (%) | Be | Mg (%) | Ca (%) | Sr | Ba | Sc | La | Y | Ti (%) | Zr | V | Cr | Mo | Mn | Fe (%) | Co | Ni | Cu | Zn | Cd | B | Al (%) | Pb | As | Sb | S (%) |
|---|---|---|---|---|---|---|---|---|---|---|---|---|---|---|---|---|---|---|---|---|---|---|---|---|---|---|---|---|
| Active-sediments | | | | | | | | | | | | | | | | | | | | | | | | | | | | |
| 1 | 0.10 | 0.28 | 1.7 | 1.25 | 1.47 | 96 | 172 | 9 | 22 | 19 | 0.12 | 31 | 110 | 33 | 4 | 3444 | 6.07 | 35 | 46 | 358 | 1388 | 6.6 | 21 | 2.98 | 42 | 317 | 7 | 0.89 |
| 2 | 0.13 | 0.29 | 1.8 | 0.99 | 2.96 | 134 | 645 | 7 | 26 | 31 | 0.12 | 23 | 78 | 23 | 1 | 1452 | 3.70 | 18 | 20 | 65 | 524 | 2.2 | 16 | 2.82 | 23 | 76 | 4 | 0.23 |
| 3 | 0.14 | 0.26 | 1.5 | 0.77 | 0.76 | 49 | 416 | 6 | 16 | 12 | 0.13 | 30 | 101 | 14 | 4 | 1339 | 5.82 | 27 | 12 | 1041 | 513 | 1.0 | 19 | 2.97 | 32 | 336 | 6 | 0.41 |
| 4 | 0.11 | 0.28 | 1.4 | 0.79 | 0.91 | 115 | 234 | 6 | 17 | 17 | 0.11 | 29 | 107 | 14 | 4 | 2018 | 6.25 | 47 | 33 | 4985 | 1105 | 4.0 | 25 | 3.37 | 43 | 460 | 6 | 0.55 |
| 5 | 0.05 | 0.12 | 4.8 | 0.42 | 1.23 | 95 | 368 | 4 | 35 | 119 | 0.04 | 10 | 35 | 15 | 15 | 3340 | 5.82 | 422 | 148 | 3736 | 3000 | 9.6 | 23 | 8.02 | 17 | 86 | 3 | 0.30 |
| 6 | 0.11 | 0.27 | 1.6 | 0.79 | 0.91 | 111 | 303 | 6 | 21 | 17 | 0.10 | 29 | 102 | 14 | 3 | 649 | 5.88 | 40 | 33 | 4480 | 1033 | 3.6 | 21 | 3.36 | 41 | 390 | 5 | 0.51 |
| 7 | 0.12 | 0.29 | 1.3 | 0.92 | 0.96 | 108 | 390 | 6 | 16 | 15 | 0.07 | 25 | 71 | 12 | 3 | 367 | 4.88 | 34 | 30 | 3407 | 880 | 2.9 | 21 | 3.24 | 36 | 352 | 5 | 0.39 |
| 8 | 0.12 | 0.28 | 1.3 | 0.96 | 1.03 | 107 | 411 | 7 | 16 | 15 | 0.10 | 29 | 79 | 15 | 4 | 538 | 4.94 | 36 | 31 | 3204 | 818 | 2.7 | 17 | 3.17 | 35 | 335 | 5 | 0.33 |
| 9 | 0.15 | 0.27 | 1.2 | 1.01 | 1.08 | 101 | 477 | 7 | 19 | 19 | 0.15 | 27 | 105 | 23 | 3 | 286 | 5.09 | 41 | 36 | 3094 | 749 | 3.3 | 16 | 3.15 | 21 | 202 | 4 | 0.27 |
| 10 | 0.05 | 0.19 | 1.4 | 0.81 | 1.11 | 41 | 249 | 7 | 28 | 32 | 0.19 | 10 | 68 | 20 | 1 | 667 | 3.31 | 17 | 14 | 80 | 251 | 0.25 | 5 | 1.90 | 23 | 35 | 1 | 0.17 |
| 11 | 0.10 | 0.26 | 1.1 | 0.96 | 0.97 | 90 | 389 | 6 | 17 | 16 | 0.12 | 27 | 91 | 20 | 2 | 1057 | 4.57 | 29 | 28 | 2237 | 626 | 1.8 | 15 | 2.77 | 25 | 190 | 3 | 0.25 |
| 12 | 0.12 | 0.22 | 1.0 | 0.96 | 1.49 | 96 | 312 | 7 | 15 | 18 | 0.14 | 18 | 117 | 22 | 2 | 1108 | 4.87 | 31 | 26 | 2413 | 564 | 1.8 | 14 | 3.17 | 17 | 150 | 3 | 0.22 |
| Average | 0.11 | 0.25 | 1.7 | 0.89 | 1.24 | 104 | 364 | 7 | 21 | 28 | 0.12 | 24 | 89 | 19 | 3.8 | 2189 | 5.10 | 65 | 38 | 2433 | 954 | 3.3 | 18 | 3.41 | 30 | 244 | 4.3 | 0.38 |
| LHL | | | | | | | | | | | | | | | | | | | | | | | | | | | | |
| T-2 | 0.17 | 0.50 | 1.5 | 0.82 | 0.64 | 223 | 76 | 9 | 17 | 17 | 0.05 | 63 | 81 | 13 | 33 | 1154 | 5.88 | 8 | 13 | 478 | 777 | 2.7 | 19 | 3.43 | 28 | 1106 | 6 | 1.32 |
| T-4 | 0.08 | 0.40 | 2.6 | 0.80 | 1.01 | 178 | 102 | 10 | 16 | 29 | 0.05 | 70 | 91 | 14 | 25 | 1425 | 8.84 | 13 | 15 | 710 | 989 | 2.5 | 24 | 3.83 | 28 | 1384 | 7 | 1.10 |
| T-5 | 0.09 | 0.26 | 3.9 | 1.00 | 1.51 | 95 | 59 | 11 | 5 | 35 | 0.05 | 75 | 77 | 10 | 12 | 7866 | 9.66 | 69 | 30 | 871 | 2538 | 7.2 | 25 | 3.78 | 24 | 2088 | 6 | 2.14 |
| Average | 0.11 | 0.39 | 3.2 | 0.87 | 1.05 | 165 | 79 | 10 | 13 | 27 | 0.05 | 69 | 83 | 12 | 23 | 3482 | 8.13 | 25.7 | 19 | 686 | 1435 | 4.1 | 23 | 3.68 | 25 | 1526 | 6.3 | 1.53 |

Concentrations in ppm exceptotherwise is indicated

**Table 5** Statistical synopsis of sediments chemical composition of the first andsecond sampling campaigns (SC-1 and SC-2, respectively)

| | Na (%) | K (%) | Be | Mg (%) | Ca (%) | Sr | Ba | Sc | La | Y | Ti (%) | Zr | V | Cr | Mo | Mn | Fe (%) | Co | Ni | Cu | Zn | Cd | B | Al (%) | Pb | As | Sb | S (%) |
|---|---|---|---|---|---|---|---|---|---|---|---|---|---|---|---|---|---|---|---|---|---|---|---|---|---|---|---|---|
| SC-1 | | | | | | | | | | | | | | | | | | | | | | | | | | | | |
| Avg | 0.11 | 0.25 | 1.68 | 0.89 | 1.24 | 103 | 364 | 6.5 | 20.7 | 27.5 | 0.12 | 24 | 89 | 18.8 | 3.8 | 2189 | 5.10 | 65 | 38 | 2433 | 954 | 3.3 | 18 | 3.41 | 30 | 244 | 4.3 | 0.38 |
| StD | 0.03 | 0.05 | 1.01 | 0.20 | 0.58 | 26.1 | 125 | 1.2 | 6.2 | 29.5 | 0.04 | 7.4 | 23.4 | 6.0 | 3.7 | 2064 | 0.93 | 113 | 36 | 1700 | 714 | 2.6 | 5.3 | 1.50 | 9.7 | 139 | 1.7 | 0.20 |
| P50 | 0.11 | 0.27 | 1.40 | 0.94 | 1.06 | 104 | 379 | 6.5 | 18 | 17.5 | 0.12 | 27 | 96 | 17.5 | 3.0 | 1495 | 5.02 | 12 | 31 | 2754 | 784 | 2.8 | 18 | 3.16 | 29 | 260 | 4.5 | 0.32 |
| IQR | 0.03 | 0.03 | 0.35 | 0.18 | 0.34 | 16.3 | 123 | 1.0 | 7.0 | 6.3 | 0.03 | 7.3 | 29.3 | 8.3 | 2.0 | 804 | 1.04 | 35 | 9.3 | 2619 | 497 | 1.9 | 5.3 | 0.34 | 14.8 | 206 | 2.3 | 0.19 |
| To, Tu, El Avg | 0.11 | 0.27 | 1.3 | 0.93 | 1.06 | 97 | 345 | 6.7 | 18 | 16 | 0.12 | 27 | 98 | 19 | 3.2 | 1572 | 5.37 | 36 | 31 | 2800 | 853 | 3.1 | 18.8 | 3.13 | 32 | 304 | 5.0 | 0.42 |
| Ll,Cl Avg | 0.09 | 0.24 | 1.6 | 0.90 | 2.04 | 88 | 447 | 7.0 | 27 | 32 | 0.16 | 17 | 73 | 22 | 1.0 | 1060 | 3.51 | 188 | 17 | 73 | 388 | 1.2 | 11.5 | 2.36 | 23 | 56 | 2.5 | 0.20 |
| In | 0.05 | 0.12 | 4.8 | 0.42 | 1.23 | 95 | 368 | 4.0 | 35 | 119 | 0.04 | 10 | 35 | 15 | 15 | 3340 | 5.82 | 422 | 148 | 3736 | 3000 | 9.6 | 23 | 8.02 | 17 | 86 | 3.0 | 0.30 |
| LHL. | 0.11 | 0.39 | 2.7 | 0.87 | 1.05 | 165 | 49 | 10 | 12.7 | 27 | 0.04 | 69 | 83 | 12 | 27 | 3482 | 8.13 | 30 | 19 | 686 | 1434 | 4.1 | 22.7 | 3.68 | 27 | 1526 | 6.3 | 0.15 |
| SC-2 | | | | | | | | | | | | | | | | | | | | | | | | | | | | |
| Av | 0.12 | 0.25 | 0.96 | 0.92 | 1.44 | 106 | 413 | 6.8 | 16.8 | 14.7 | 0.15 | 33 | 112 | 17.0 | 1.8 | 969 | 4.94 | 23 | 18 | 1169 | 405 | 1.3 | 14.2 | 2.51 | 24 | 161 | 3.6 | 0.35 |
| StD | 0.03 | 0.05 | 0.19 | 0.16 | 0.46 | 24.5 | 117 | 0.4 | 4.9 | 5.9 | 0.06 | 9.8 | 52.2 | 2.6 | 0.93 | 354 | 1.53 | 6 | 4.2 | 733 | 170 | 0.7 | 2.3 | 0.42 | 5.7 | 87 | 1.6 | 0.16 |
| P50 | 0.12 | 0.24 | 1.00 | 0.89 | 1.36 | 114 | 420 | 7.0 | 16 | 13.0 | 0.12 | 36 | 89 | 17 | 2.0 | 930 | 4.35 | 24 | 19 | 1374 | 459 | 1.5 | 14 | 2.56 | 24 | 148 | 3.0 | 0.33 |
| IQR | 0.02 | 0.08 | 0.20 | 0.30 | 0.25 | 19.0 | 139 | 0.0 | 1.5 | 2.5 | 0.06 | 7.5 | 28.0 | 3.5 | 1.5 | 246 | 0.71 | 8.0 | 7.0 | 1062 | 247 | 0.8 | 2.5 | 0.55 | 10 | 44 | 0.5 | 0.09 |
| %V 1–2 | 4.3 | 0.0 | 27.3 | 1.7 | 7.5 | 1.4 | 6.3 | 2.3 | 10.4 | 30.3 | 11.1 | 15.8 | 11.4 | 5.0 | 35.7 | 38.6 | 1.6 | 47.7 | 35.7 | 35.1 | 40.4 | 43.5 | 11.8 | 15.2 | 11.1 | 20.5 | 8.9 | 4.1 |
| Sed Avg | 0.57 | 2.0 | 2.0 | 1.4 | 6.6 | 320 | 460 | 10 | 41 | 40 | 0.38 | 150 | 105 | 72 | 2 | 770 | 4.1 | 14 | 52 | 33 | 95 | 0.17 | 100 | 7.2 | 19 | 7.7 | 1.2 | 0.22 |
| Crust Avg | 2.3 | 0.91 | | 3.2 | 5.3 | 260 | 250 | 30 | 16 | 20 | 0.54 | | 230 | 185 | 1 | 1400 | 7.07 | 29 | 105 | 75 | 80 | 0.1 | | 8.4 | 8.0 | 1.0 | | 0.03 |

Contents in ppm except% is noted; Avg: average; Std: standard deviation; P50: median (percentile 50);IQR: Interquartile range (Percentile 75-Percentile 25); %V1-2: Variationpercentage between SC-1 and SC-2 (100*[highervalue-average]/average)

To, Tu, El Avg: Average of the Toro, Turbio and Elqui river samples; Ll, Cl Avg: Average of the La Laguna and Claro river samples; In: Incaguaz river sample; LHL: Lower Holocene Layer samples; Sed Avg: Worldwide average of sediments (Sparks 1995); Crust Avg: Crustal average (Lof 1987)

**Table 6** Reference values for chemical composition of river sediments (in ppm, except Fe and S, in %)

| Source | Constituent | | | | | | | | | | | |
|---|---|---|---|---|---|---|---|---|---|---|---|---|
| | Sc | Mn | Fe | Co | Ni | Mo | Cu | Zn | Cd | Pb | As | S |
| Elqui River sediments[1] | | 1151 | | 18 | 12 | 1 | 1077 | 326 | 1.2 | 26 | 106 | |
| Elqui River sediments[2] | | | 4.9 | | | | 2352 | 470 | | | 202 | |
| Elqui River sediments[3] | | | | | | 2.6 | 1420 | 492 | 1.6 | 28 | 133 | 0.28 |
| Elqui River sediments[4] | 5.7 | 1725 | 4.5 | 30 | 21 | 2.0 | 1412 | 428 | 1.4 | 31 | 112 | 0.27 |
| Atacama andean basins[5] | | | | | | 1.9 | 207 | | 0.9 | | 162 | |
| Current study, first sampling | 6.5 | 2189 | 5.1 | 65 | 38 | 3.8 | 2433 | 954 | 3.3 | 30 | 244 | 0.38 |
| Current sydy, second sampling | 6.8 | 969 | 4.9 | 23 | 18 | 1.8 | 1169 | 405 | 1.3 | 24 | 161 | 0.35 |
| Current study, Lower Holocene terrace | 10 | 3482 | 8.1 | 30 | 19 | 27 | 686 | 1434 | 4.1 | 27 | 1526 | 1.53 |
| Sediment worldAverage[6] | 10 | 770 | 4.1 | 14 | 52 | 2 | 33 | 95 | 0.2 | 19 | 7.7 | 0.22 |
| Crustal average[7] | 30 | 1400 | 7.1 | 29 | 105 | 1 | 75 | 80 | 0.1 | 8 | 1 | 0.03 |

[1]Oyarzún et al. (2003); [2]Oyarzun et al. (2004); [3]Oyarzún et al. (2012); [4]Oyarzún et al. (2016); [5]Tapia et al. (2018); [6]Sparks (1995); [7]Lof (1987)

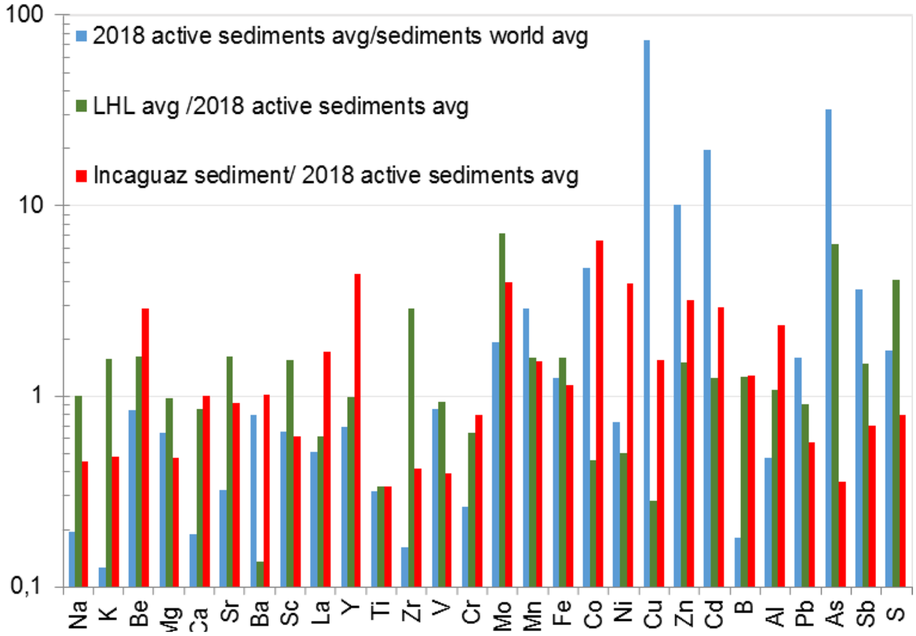

**Fig. 3** Sediment's concentration ratios between average (avg) of 2018 (active sediments), LHL, Incaguaz, and World's reference figures from Sparks (1995)

subgroups were identified: (a) Mn, Zn, Fe, Cu, K, and Al, and (b) Ca, As, Na, and Mg.

The results of the sediments' chemical analysis are presented in Table 4 and the statistical parameters and a comparison with the second sampling results are shown in Table 5. The elements' average concentrations in the first and second samplings are similar (differences < 20%) for 18 elements, most of them not linked to ARD. In contrast, 10 elements presented differences > 20%, 7 of them related to ARD (Mo, Mn, Co, Cu, Cd, As), which attained higher levels in the Sept. 2018 sampling. The active sediments of the Toro and Turbio rivers, and to a moderate degree those of the Elqui River, are clearly enriched in Cu, Zn, Cd, and As. In exchange, those elements present moderate concentrations in the Laguna and Claro sediments. Finally, the Incaguaz river sediments are high in Cu and Zn, but low in As. They are also enriched in Be, Y, Mo, and Co. The fact that the water in this river is alkaline and presents low sulfate and As levels suggests the presence of mineralization not yet recognized in that basin.

Comparison of the new spectrographic data for active sediments with the figures from previous studies (Table 6) shows good agreement. Compared to the Sparks (1995) world averages for river sediments (Fig. 3) and the Earth's crust (Lof 1987), the high Cu, Zn, Cd, and As of the active sediments of the Toro, Turbio and Elqui Rivers stand out. On the other hand, Sc, Mn, Fe, Co, Ni, and Mo are in the same order of magnitude. In comparison to the Andean sediments of the neighboring Atacama basin (Tapia et al. 2018), Mo, Cd, Cd, and As contents are similar, but Cu is 9–10 times higher in the Toro-Turbio-Elqui sediments. The metal contents of the LHL confirm that their origin is related to ARD, although it differs from the current active sediment composition with greater As, Mo, and S, and lesser Cu contents. This difference is probably related to the deposit formation and physicochemical evolution in the organic matter rich bottom of an ephemeral lake in the Turbio river course, which affects both mineralogy and chemical composition. Mn, Fe, Cu, Zn, and As contents of active and LHL sediments are compared in Fig. 4.

The relationships between sediment and water samples for Cu, Zn, As and Mn are presented in Fig. 5. A similar behavior between the concentrations in both sediments and waters is observed, except for the Incaguaz River (5), which presents high Cu and Zn contents in sediment but low concentrations in water.

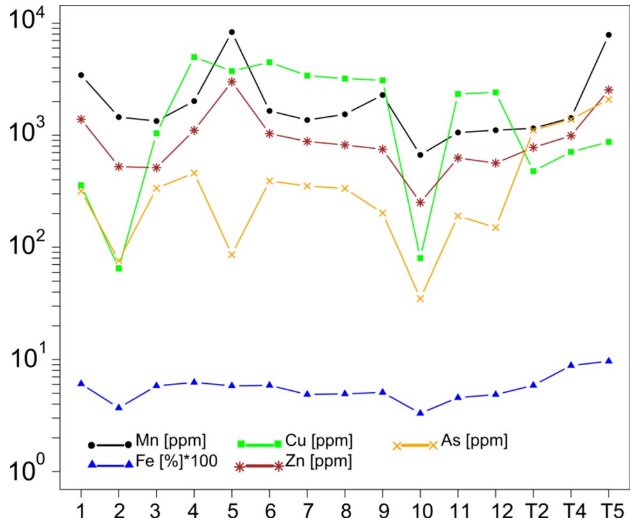

**Fig. 4** Chemical composition of active (1–12) and LHL (T2–T5) sediments

*Sequential extractions tests*. Figure 6 shows the average results of the extractions for the active and LHL sediment samples. With an estimation error up to 10–20%, these results should be considered as semi-quantitative only.

Different chemical patterns were identified. For example, Mg, Ti, V, Cr, Fe, Al, and As in the active sediments, and Sr in the LHL samples presented minor or no response to the extractions. This behavior is similar to that described by Copaja et al. (2014) for Fe, Al, and Cr in fluvial sediments in the neighboring Choapa river basin. This could be due to the presence of mineralogical phases that are refractory to dissolution such as ferromagnesian silicate or iron oxides such as magnetite. An additional possible cause is their inclusion by coprecipitation in refractory iron ochre (oxyhydroxides) precipitates, such as As in goethite, as previously detected in the LHL by Oyarzun et al. (2004) using ESEM-EDX analysis, and by Tapia et al. (2018) in river sediments of the Atacama Region.

A second pattern was displayed by the elements that were leached by the extraction methods, but behaved differently in the selective dissolutions in acidic, and acid-reducing and -oxidizing conditions. The extraction percentage was greater in the LHL sediments, except for Cu and Zn. The most consistent responses were those of Ca, Zn, and Cd to acidic extraction, and that of Y to acid-oxidizing extraction. Meanwhile, Cu responded mainly to acidic extraction in active sediments but to acid-oxidizing extraction in the LHL. Of special interest is the association of Co and Ni with Mn in the acid-reducing extraction. This is thought to be a result of the reduction of $MnO_2$ to the $Mn^{2+}$ state, which releases those elements that were adsorbed when oxidation and hydrolysis of $Mn^{2+}$ took place (Sahoo et al. 2012; Singh et al. 1984). Regarding sulfur in the active sediments, it responded mainly to the acid-oxidizing extraction, due to its presence as pyrite. Meanwhile, it is found as gypsum in the LHL, which explains its dissolution in the first extraction stage.

How does all this relate to the environmental conditions in the Elqui watershed? Under the present conditions, the stability of metals in the fine sediment fraction could be only locally affected (e.g. release of Mn and associated elements such as Co, Ni, Cu, Zn, and Cd in the reduced environments of the lower Elqui river meadows). On the other hand, a favorable outcome of the extraction tests is the refractory behavior of arsenic, considering that this element is very much the most toxic chemical species of the basin. However, extreme flood events related to “Mega-Niño” (ENSO) episodes (Keefer et al. 2003) could trigger the massive removal of those metals currently precipitated by hydrolytic reactions.

## Conclusions

The El Indio district has been a source of major ARD for at least ten thousand years in the Toro River subbasin. This natural acidic generation process was enhanced during the underground mining of the Au-Cu-As ores (1975–2002). However, the arid conditions of the Elqui basin have prevented the ARD from having potentially worse effects on the waters of the Turbio and Elqui rivers. This is due to the hydrolytic and precipitation reactions produced by the mixing of the acidic, metal- and As-rich waters of the Toro River with the alkaline waters of the La Laguna River (at the onset of the Turbio River). The alkalinity of the Turbio River is reinforced downstream by the inputs of the Incaguaz and Claro rivers. Thus, although the Cu, Zn, and As fine sediments contents of the Turbio and Elqui rivers are clearly anomalous, the metal and As contents of their waters have

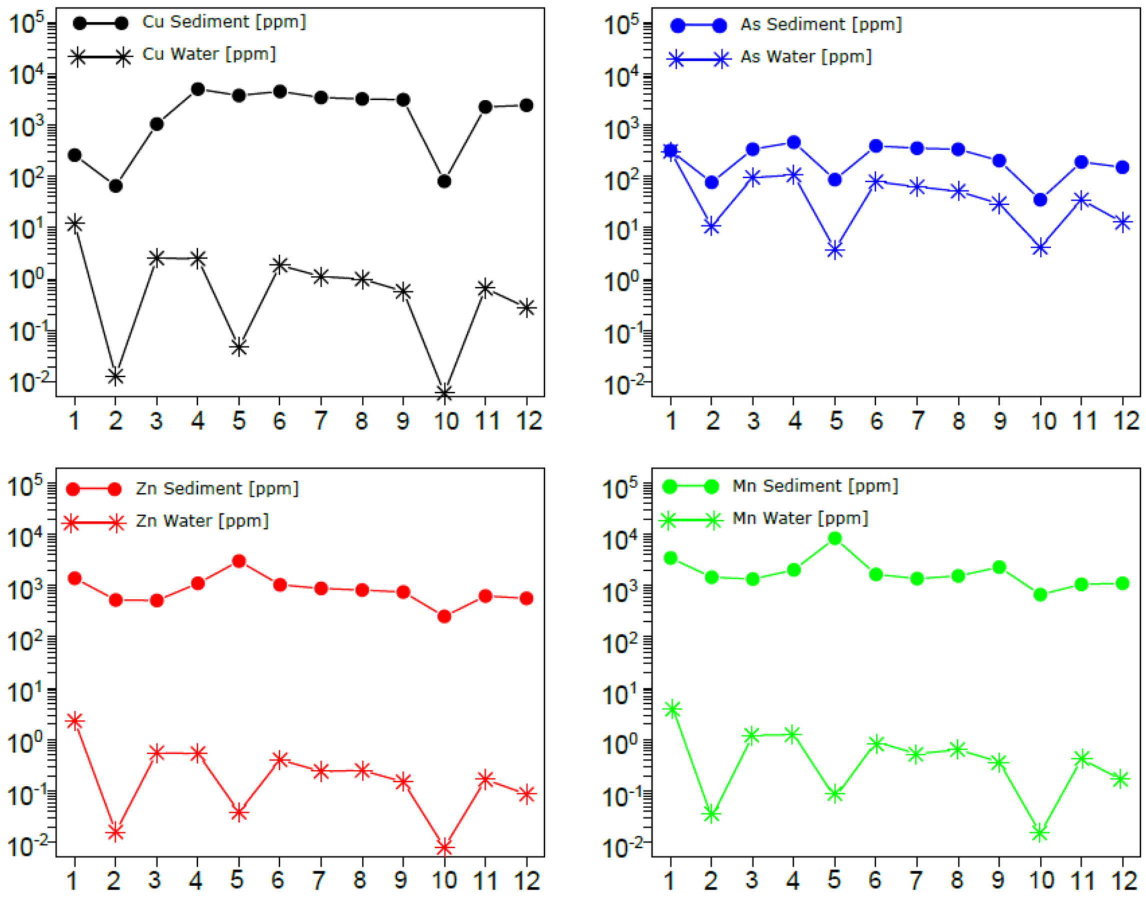

**Fig. 5** Active sediments and water chemical composition for selected elements

been compatible with agricultural and human consumption. However, the hydrolytic process implies that large amounts of Cu, Zn, As and other metals are present and continue to accumulate in the fine fraction of the Turbio and Elqui rivers sediments. Also, the Puclaro dam is accumulating As and Cu as a consequence of its originally unforeseen role as a sink for particle-bound metals. These unique conditions motivated the experimental component of the present study, i.e. to assess the risks that some of these metals could be remobilized by changes in physical-chemical conditions related to local events or climate change.

The results of the sequential extraction tests defined two main behavioral types. One group of elements, including Mg, Ti, V, Cr, Fe, and As presented little response to the different extraction conditions. A second group (Cu, Zn, Cd, and other elements), were more susceptible to acidic selective dissolution, whereas Mn, Co, and Ni responded to reducing acidic conditions. From the point of view of environmental risk, the favorable result is that potentially toxic elements like As, V, and Cr were refractive to the tested conditions. In the case of As, its stability with respect to the acid-reducing extraction was unexpected, considering its assumed association with Fe-oxyhydroxide.

The new sediment and water samplings and the expansion of the range of analyzed elements allowed the detection of elevated Li levels, which in the Toro River surpassed 800 μgL$^{-1}$ and in the Turbio 330 μgL$^{-1}$, far above the worldwide average level in river waters (ca. 1–20 μgL$^{-1}$). Last but not least, the finding of high Co, Ni, Y, and Mo contents (together with Cu and Zn) in the sediments of the Incaguaz River defines a striking geochemical anomaly that may be indicating the presence of a low-sulfur type of mineralization.

**Acknowledgements** This work was developed within the framework of the ANID/FONDECYT/1180153, the Water Resources and Environment Program (PRHIMA, for its acronym in Spanish) of the Department of Mining Engineering of Universidad de La Serena, ANID/FONDAP/15130015, and ANID/FONDAP 15110020. The paper benefitted from the comments of two anonymous reviewers, and Drs. B. Plante (Associate Editor) and R. Kleinmann (Editor-in-chief), who we thank.

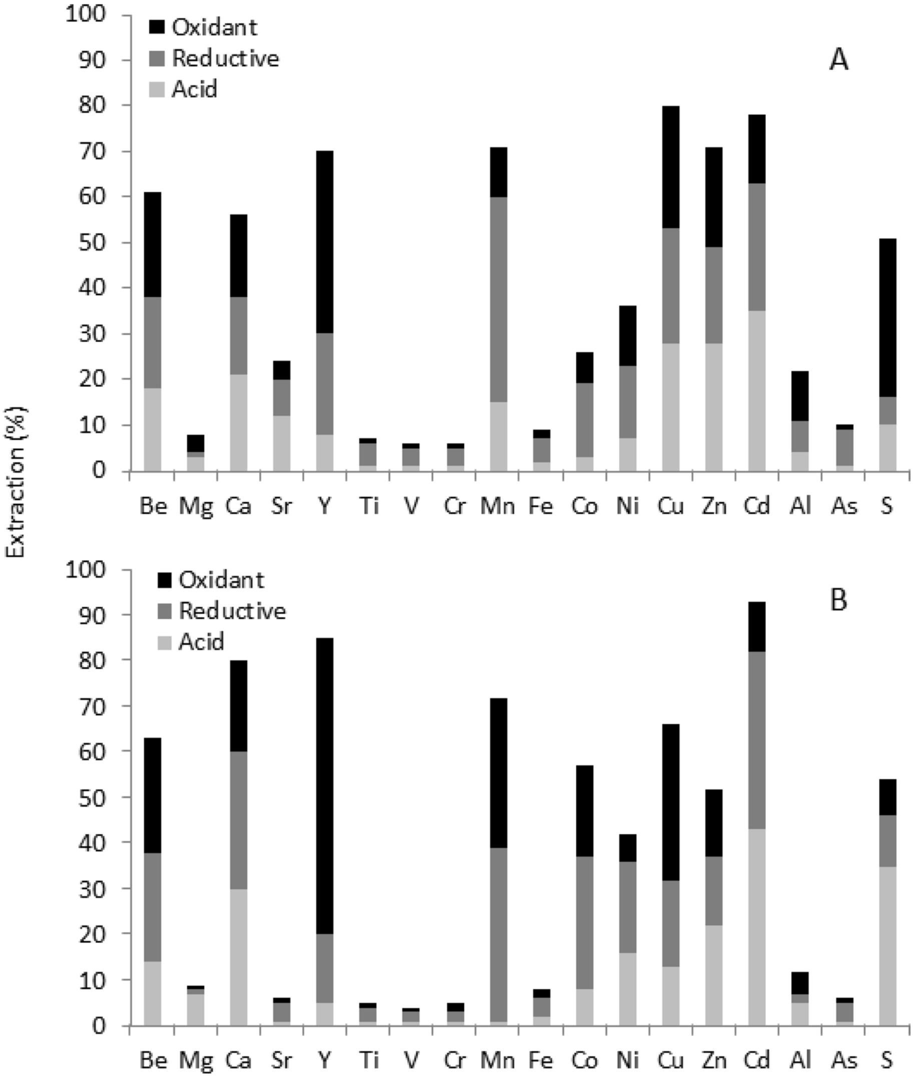

**Fig. 6** Adjusted results (%) for different extraction conditions in active (A) and LHL (B) sediments

## References

Bissig T, Clark AH, Lee JKW, von Quadt A (2003) Petrogenetic and metallogenetic responses to Miocene slab flattening: new constraints from the El Indio-Pascua Au-Ag-Cu belt, Chile/Argentina. Miner Depos 38:844–862

Brown GE, Hochella MF, Calas G (2017) Improving mitigation of the long-term legacy of mining activities: Nano- and molecular-level concepts and methods. Elements 13(5):325–330

Bugueño M, Acevedo S, Bonilla C, Pizarro G, Pasten P (2014) Differential arsenic binding in the sediments of two sites in Chile's lower Loa River basin. Sci Total Environ 466:387–396

Caraballo MA, Serna A, Macías F, Pérez-López R, Cánovas-Ruiz C, Richter P, Becerra-Herrera M (2018) Uncertainty in the measurements of toxic metals mobility in mining/mineral wastes by standardized BCR®SEP. J Hazard Mater 360:587–593

Contreras MT, Mullendorff D, Pasten P, Pizarro GE, Paola C, Escauriaza C (2015) Potential accumulation of contaminated sediments in a reservoir of a high-Andean watershed: Morphodynamic connections with geochemical processes. Water Resour Res 51(5):3181–3192

Copaja S, Molina X, Tessada R (2014) Determination of heavy metals in Choapa river sediments using BCR sequential extraction procedure. J Chil Chem Soc 59(1):2353–2358

Favier V, Falvey M, Rabatel A, Praderio E, López D (2009) Interpreting discrepancies between discharge and precipitation in high-altitude area of Chile's Norte Chico region (26–32ºS). Water Resour Res 45:W02424. doi:https://doi.org/10.1029/2008WR006802

Galleguillos G, Oyarzún J, Maturana H, Oyarzún R (2008) Retención de arsénico en embalses: El caso del Rio Elqui, Chile. Tecnol y Cienc del Agua 23:29–36

Guerra P, Gonzalez C, Escauriaza C, Pizarro G, Pastén P (2016) Incomplete mixing in the fate and transport of arsenic at a river affected by acid drainage. Water Air Soil Pollut. https://doi.org/10.1007/s11270-016-2767-5

Heather KB, Bissig T, Staff of Exploraciones Barrick Chile Ltda (2003) Regional Geology of the El Indio Mineral District, North-central Chile. 10° Congreso Geológico Chileno. Universidad de Concepción, Concepción, Chile (CD-ROM)

Jannas RR, Beane RE, Ahler BA, Brosnahan DR (1990) Gold and copper mineralization at El Indio deposit, Chile. J Geochem Explor 36:233–266

Jannas RR, Bowers TS, Petersen U, Beane RE (1999) High-sulfidation deposit types in the el Indio district, Chile. In: Skinner BJ (ed)

Geology and Ore Deposits of the Central Andes Vol, 7. Society of Economic Geologists Special Publication, pp 219–266

Kavanagh L, Keohane J, Cleary J, García-Cabellos G, Lloyd A (2017) Lithium in the natural waters of the south east of Ireland. Int J Environ Res Public Health 14(6):561–577

Keefer D, Moseley ME, deFrance SD (2003) A 38,000-year record of floods and debris flows in the IIo region of southern Peru and its relation to El Niño events and great earthquakes. Palaeogeogr Palaeoclimatol Palaeoecol 194(1–3):41–77

Levinson AA (1974) Introduction to Exploration Geochemistry. Applied Publishing Ltd, Maywood

Lof P (1987) Elsevier's Periodic Table of the Elements. Elsevier Publishers, The Netherlands

Maksaev V, Townley B, Palacios C, Camus F (2007) Metallic ore deposits. In: Moreno T, Gibbons W (eds) The Geology of Chile. The Geological Society of London, pp 179–199

Maturana H, Oyarzún J, Valencia W (1995) Estimación del potencial de drenaje ácido de la mina Río del Medio y sus desmontes. Universidad de La Serena, Report for Compañía Minera El Indio

Maturana H, Oyarzún J, Valencia W, Gaete M (1996) Contenidos de arsénico en los suelos del distrito minero El Indio, con referencia a su origen natural o antrópico. Universidad de La Serena, report for Compañía Minera El Indio

Montecinos M, Coquery M, Alsina MA, Bretier M, Gaillard JF, Dabrin A, Pasten P (2020) Partitioning of copper at the confluences of Andean rivers. Chemosphere. https://doi.org/10.1016/j.chemosphere.2020.127318

Narváez P (1970) Antecedentes sobre la zona de alteración El Indio. Internal report, National Mining Company (ENAMI)

Nordstrom DK (2011) Hydrogeochemical processes governing the origin, transport, and fate of major and trace elements from mine wastes and mineralized rocks to surface waters. Appl Geochem 26(11):1777–1791

Nowrouzi M, Pourkhabbaz A (2014) Application of geoaccumulation index and enrichment factor for assessing metal contamination in the sediments of Hara Biosphere Reserve. Iran Chem Spec Bioavailab 26(2):99–105

Núñez J, Rivera D, Oyarzún R, Arumí JL (2013) Influence of Pacific Ocean multidecadal variability on the distributional properties of hydrological variables in north-central Chile. J Hydrol 501:227–240. doi:https://doi.org/10.1016/j.jhydrol.2013.07.035

Oyarzun R, Ortega L, Sierra J, Lunar R, Oyarzún J (1998) Cu, Mn, and Ag mineralization in the Quebrada Marquesa Quadrangle, Chile: the Talcuna and Arqueros districts. Miner Depos 33:547–559

Oyarzun R, Lillo J, Higueras P, Oyarzún J, Maturana H (2004) Strong arsenic enrichment in sediments from the Elqui watershed, northern Chile: industrial (gold mining at El Indio-Tambo district) vs. geologic processes. J Geochem Explor 84:53–64

Oyarzun R, Guevara S, Oyarzún J, Lillo J, Maturana H, Higueras P (2006) The As-contaminated Elqui river basin: a long lasting perspective (1975–1995) covering the initiation and development of Au-Cu-As mining in the high Andes of northern Chile. Environ Geochem Hlth 28:431–443

Oyarzun R, Lillo J, Oyarzún J, Higueras P (2007a) Plate interactions, evolving magmatic styles, and inheritance of structural paths: development of the goldrich, Miocene El Indio Epithermal Belt, northern Chile. Int Geol Rev 49:844–853

Oyarzun R, Lillo J, Oyarzún J, Maturana H, Higueras P (2007b) Mineral deposits and Cu-Zn-As dispersion - contamination in stream sediments from the semiarid Coquimbo Region, Chile. Environ Geol 53:283–294

Oyarzún J, Maturana H, Paulo A, Pasieczna A (2003) Heavy metals in stream sediments from the Coquimbo region (Chile): effects of sustained mining and natural processes in a semi-arid Andean basin. Mine Water Environ 22:155–161

Oyarzún J, Castillo D, Maturana H, Kretschmer N, Soto G, Amezaga J, Rötting TS, Younger PL, Oyarzún R (2012) Abandoned tailings deposits, acid drainage and alluvial sediments geochemistry, in the arid Elqui River Basin, north-central Chile. J Geochem Explor 115:47–58

Oyarzún J, Carvajal MJ, Maturana H, Núñez J, Kretschmer N, Amézaga J, Rötting T, Strauch G, Thyne G, Oyarzún R (2013) Hydrochemical and isotopical patterns in a calc-alkaline Cu- and Au-rich arid Andean Basin: the Elqui River watershed, north central Chile. Appl Geochem 33:50–63

Oyarzún J, Oyarzun R, Lillo J, Higueras P, Maturana H, Oyarzún R (2016) Distribution of chemical elements in calc-alkaline igneous rocks, soils, sediments and tailings deposits in northern central Chile. J S Am Earth Sci 69:25–42

Oyarzún J, Núñez J, Maturana H, Oyarzún R (2018) The El Indio mine closure plan effects over the water quality of the upper Elqui Basin. Environ Eng Geosci 24(3):349–355

Parra A, Oyarzún J, Maturana H, Kretschmer N, Meza F, Oyarzún R (2011) Natural factors and mining activity bearings on the water quality of the Choapa basin, north Central Chile: insights on the role of mafic volcanic rocks in the buffering of the acid drainage process. Environ Monit Assess 181:69–82

Reich M, Parada MA, Palacios C, Dietrich A, Schultz F, Lehmann B (2013) Adakite-like signature of Late Miocene intrusions at the Los Pelambres giant porphyry copper deposit in the Andes of central Chile: metallogenic implications. Miner Depos 38(7):876–885

Rice EW, Baird RB, Eaton AD (2017) Standard Methods for the Examination of Water and Wastewater, 23rd edit, American Public Health Assoc, American Water Works Assoc, Water Environment Federation

Sahoo PK, Tripathy S, Panigrahi MK, Equeenudddin SM (2012) Mineralogy of Fe-precipitates and their role in metal retention from and acid mine drainage site in India. Mine Water Environ 31:344–352

Scaff L, Rutllant JA, Rahn D, Gascoin S, Rondanelli R (2017) Meteorological interpretation of orographic precipitation gradients along an Andes west slope basin at 30 ºS (Elqui Valley, Chile). J Hydrometeorol 18:713–727. doi:https://doi.org/10.1175/JHMD-16-0073.1

Singh S, Subramanian V, Gibbs RJ (1984) Hydrous Fe and Mn oxides — scavengers of heavy metals in the aquatic environment. Crit Rev Env Control 14(1):33–90

Sparks DL (1995) Environmental Soil Chemistry. Academic Press, New York

Tapia J, Davenport J, Townley B, Dorador C, Schneider B, Tolorza V, von Tümpling W (2018) Sources, enrichment, and redistribution of As, Cd, Cu, Li, Mo, and Sb in the northern Atacama Region, Chile: implications for arid watersheds affected by mining. J Geochem Explor 185:33–51

Zavala H (2006) Hidrología del humedal Tambo-Puquios. In: Cepeda J (ed) Geoecología de los Andes Desérticos La Alta Montaña del valle de Elqui. Ediciones Universidad de La Serena, La Serena, pp 285–323